

Study of Low-Temperature Heat Accumulation in Sensible and Latent Thermal Energy Storage Systems for Greenhouse Applications

Mukminov I., Pysarevskiy I., Volgusheva N., Boshkova I., Verkhivker Ya., Altman E.

Odesa National University of Technology

Odesa, Ukraine

Abstract. The main objective of this study is to determine the energy efficiency of a sensible heat storage system employing a dense crushed stone bed in a vertical heat exchange channel, as well as a latent heat storage system using a phase change material based on paraffin T3, intended for greenhouse applications. To achieve this objective, several tasks were performed, including analytical and experimental investigation of heat transfer processes in thermal energy storage system elements using a greenhouse model, analysis of the temporal variation of temperature profiles and solar radiation intensity, and a comparative evaluation of the energy efficiency of phase change heat storage materials, represented by modified paraffin, and capacitive heat storage systems, represented by crushed stone. The most significant results demonstrate that the derived analytical relationships for calculating working medium temperatures adequately describe the physical process of heat accumulation when experimental heat transfer coefficients are considered. Heat exchange between the dense crushed stone bed and the water flow occurs with high intensity, with an average heat transfer coefficient of $\alpha = 80 \text{ W}/(\text{m}^2 \cdot \text{K})$. The emissivity of the surface of paraffin-filled heat storage tubes was determined to be $\varepsilon_p = 0.65$. The significance of the results lies in defining conditions for efficient application of thermal energy storage systems in greenhouse practice. For thermal stabilization of the internal greenhouse volume, the use of modified paraffin T3 is recommended, as its heat storage efficiency is 7.5–9.3 times higher than that of a dense crushed stone bed.

Keywords: heat transfer, solar radiation, greenhouse, phase change material, dense crushed stone bed, temperature, efficiency, thermal energy storage.

DOI: <https://doi.org/10.52254/1857-0070.2026.1-69.07>

UDC: 620.92:536.24:631.544

Studiul acumulării căldurii cu potențial termic scăzut în sistemele de stocare a căldurii sensibile și latente în sere

Mukiminov I.I., Pisarevsky I.A., Volgusheva N.V., Boškova I.L., Verhivker Ya.G., Altman E.I.

Universitatea Națională de Tehnologie din Odesa, Odesa, Ucraina

Rezumat. Scopul principal al acestui studiu este determinarea eficienței energetice a sistemului de acumulare a căldurii sensibile utilizând un strat dens de piatră spartă într-un canal vertical de schimb de căldură, precum și a sistemului de acumulare a căldurii latente utilizând un material cu schimbare de fază pe bază de parafină T3, pentru aplicații în sere. Pentru atingerea acestor obiective au fost realizate următoarele sarcini: studiul analitic și experimental al proceselor de transfer de căldură în elementele sistemelor de acumulare a căldurii utilizând un model de seră; analiza variației în timp a curbelor de temperatură și a intensității radiației solare; precum și evaluarea comparativă a eficienței energetice a materialelor de acumulare a căldurii cu schimbare de fază, exemplificată prin parafină modificată, și a sistemelor capacitive de acumulare a căldurii, exemplificate prin piatră spartă. Cele mai importante rezultate obținute sunt următoarele: dependențele analitice pentru calculul temperaturilor mediilor de lucru descriu în mod adecvat procesul fizic de acumulare a căldurii, ținând cont de datele experimentale privind coeficienții de transfer de căldură; schimbul de căldură dintre stratul dens de piatră spartă și fluxul de apă are loc cu o intensitate ridicată, coeficientul mediu de transfer de căldură fiind $\alpha = 80 \text{ W}/(\text{m}^2 \cdot \text{K})$; capacitatea de emisie a suprafeței tuburilor de acumulare a căldurii cu parafină este $\varepsilon_p = 0.65$. Semnificația rezultatelor obținute constă în determinarea condițiilor de utilizare eficientă a sistemelor de acumulare a căldurii pentru exploatarea de sere. În special, pentru stabilizarea termică a volumului interior al modelului de seră, este recomandată utilizarea parafinei modificate T3, eficiența acumulării căldurii fiind de 7.5–9.3 ori mai mare comparativ cu stratul dens de piatră spartă.

Cuvinte-cheie: transfer de căldură, radiație solară, seră, material cu schimbare de fază, strat dens de piatră spartă, temperatură, eficiență, stocarea energiei termice.

Исследование аккумуляции теплоты низкого температурного потенциала в системах хранения явного и скрытого тепла для тепличных хозяйств

Мукминов И.И., Писаревский И.А., Волгушева Н.В., Бошкова И.Л., Верхивкер Я.Г., Альтман Э.И.
Одесский национальный технологический университет

Одесса, Украина

Аннотация. Основной целью работы является определение энергетических характеристик работы систем хранения тепла явного типа при использовании плотного слоя щебня в вертикальном теплообменном канале и скрытого тепла при использовании фазопереходного материала на основе парафина ТЗ для тепличных хозяйств. Для достижения поставленных целей были решены следующие задачи: определение условий применимости аналитических зависимостей для расчета локальных температур теплоаккумулирующих материалов; экспериментальное исследование процессов нестационарного теплообмена в элементах теплоаккумулирующих систем на макете теплицы; анализ кривых зависимости температуры рабочих тел и интенсивности солнечного излучения от времени; проведение сравнительной оценки энергетической эффективности применения фазопереходных теплоаккумулирующих материалов на примере модифицированного парафина и емкостных накопителей теплоты в явном виде на примере щебня. Наиболее важными результатами являются: аналитические зависимости для расчета температур рабочих тел адекватно описывают физический процесс аккумуляции теплоты при учете экспериментальных данных по коэффициентам переноса; теплообмен между плотным слоем щебня и потоком воды проходит с высокой интенсивностью, средний коэффициент межкомпонентного теплообмена $\alpha=80 \text{ Вт}/(\text{м}^2\cdot\text{К})$; модифицированный парафин ТЗ как фазопереходный материал в 7.5–9.3 раза эффективнее аккумулирует низкопотенциальную теплоту солнечного излучения и воздуха в макете теплицы в сравнении с плотным слоем щебня; степень черноты поверхности аккумулирующих трубок с парафином составляет $\varepsilon_p=0.65$. Значимость полученных результатов заключается в определении условий эффективного использования теплоаккумулирующих систем для тепличных хозяйств. В частности, для термостабилизации внутреннего объема макета теплицы обосновано применение модифицированного парафина ТЗ. Проблема гидравлического сопротивления слоя гранулированного материала, используемого в качестве теплообменной насадки в тепловых аккумуляторах явной теплоты, решается вертикальным расположением канала и организацией теплообмена с потоком воды, нагревающейся от низкопотенциальных источников теплоты.

Ключевые слова: теплообмен, солнечное излучение, теплица, фазопереходный материал, плотный слой щебня, температура, эффективность, хранение тепловой энергии.

INTRODUCTION

The process of energy accumulation plays a key role in the storage of electrical and thermal energy from renewable sources—wind, solar, and wave energy—thereby enabling the decarbonization of the power sector [1]. The utilization of thermal energy offers the most promising opportunities to balance supply and demand by overcoming the intermittency and instability of real heat sources, leading to the development of a more flexible, resilient, and reliable energy system [2]. Review [3] presents a critical analysis of advances in the field of energy storage systems from 1850 to 2022, including their evolution, classification, and operating principles. Traditionally, low-grade thermal energy has been neglected and discharged into the environment, resulting in low overall energy efficiency [4]. As a consequence, in recent years there has been increased interest in the utilization of low-grade thermal energy, with research increasingly focusing on the development of appropriate technologies and application methods for this energy resource [4, 5]. In study [6],

significant advances in electrochemical, mechanical, chemical, and thermal energy storage systems are reported, highlighting their important role in addressing intermittently arising challenges associated with renewable energy sources such as solar and wind energy. Thermal energy storage technologies are developing along two main directions: storage of thermal energy in sensible form (capacity-type storage), manifested by a change in the temperature of the material, or in latent form during a phase transition, such as melting or boiling [7]. Sensible heat storage units utilize the heat capacity of the storage material, which is heated or cooled without a change in its physical state [8].

The advantages of sensible heat storage (SHS) systems include simplicity of design, moderate thermal conductivity, and lower cost of the storage material; however, they are limited by a relatively low energy storage density, which additionally increases the size of the storage system. Technologies based on heat storage via heat capacity employ readily available materials,

such as solid rocks in the form of crushed stone or stones [9, 10].

Latent heat storage (LHS) systems offer advantages such as higher energy storage density, the ability to maintain temperature at a specified level, and compact size. However, in terms of the rate of heat propagation within the material layer, LHS systems are significantly inferior to SHS systems and are therefore scarcely used for commercial applications. A substantial enhancement of heat transfer can be achieved by adding nanoparticles with higher thermal conductivity to phase change materials (PCMs) [11]. However, it is noted that their widespread application may give rise to environmental concerns, as improper disposal can lead to toxicity and cause harm to ecosystems. Thus, despite significant progress in understanding the thermophysical properties and operational performance of nanofluids, challenges remain in achieving long-term stability, minimizing environmental impact, and improving economic viability.

For the utilization of waste heat from industrial processes, thermal energy storage systems employing packed beds of granular materials are used. Such systems can be applied for storing excess heat and releasing it as required [12]. Heat exchangers with granular beds are successfully utilized in many industrial fields. In study [13], a novel configuration using a granular material layer for sensible heat storage was proposed as a thermal energy storage (TES) system for a concentrated solar power plant. It was found that the optimal dimensions of the bed strongly depend on the particle size of the granular material, since this parameter has a significant effect on the fluid pressure drop. The magnitude of the pressure drop of the flowing gas is of critical importance in the design of regenerative heat exchangers or devices employing a packed or structured material bed. The dominant operational costs are associated with the pumping of circulating air, which depend on the pressure drop across the bed [14].

For the effective application of energy storage technologies based on granular materials, a number of parameters must be taken into account, including scale, storage duration and period of the stored energy, operating temperature range, capacity range, energy density, and recharge time [14]. Another determining aspect is the particle size forming the material bed. Pressure drop can be reduced by using materials with larger particle

sizes; however, this may lead to a deterioration of thermal performance [15].

PCM-based storage units are more efficient [16] than capacity-type storage systems, since the enthalpy of phase transition is significantly higher than sensible heat content. In TES systems, solid-liquid phase transitions are most commonly employed. The melting temperature, latent heat of fusion, and thermophysical properties of the PCM are the three main factors influencing material selection for a specific application [17]. Numerous mechanical and nanotechnological enhancements aimed at increasing the heat transfer rate have been achieved, which appears promising. Most of the literature focuses on standard and commercially available PCMs, such as paraffin.

The authors of [18] demonstrated that combining sensible and latent thermal energy storage materials (TESMs) makes it possible to exploit the properties of different materials, compensating for the performance limitations of individual materials and improving the overall performance of thermal heat storage (THS) systems. An innovative combined sensible-latent THS system employing concrete spheres as sensible TEsMs and paraffin-encapsulated capsules as latent TEsMs [19] outperformed purely sensible heat storage systems, exhibiting superior thermal characteristics as well as higher energy storage capacity and outlet temperature.

The accumulation and utilization of excess solar energy in greenhouses to smooth air temperature fluctuations is one of the approaches to increasing energy efficiency and reducing energy consumption. Greenhouse production is the most energy-intensive and costly segment of the agricultural sector [20]. Therefore, increasing attention is being paid to the development of design solutions for environmentally friendly and energy-efficient greenhouses. The application of solar energy storage units for greenhouse heating has proven to be promising [21]. Of particular interest are regenerators in which a dense bed of granular (bulk) materials is used as the storage medium [22]. Owing to the highly developed heat transfer surface, represented by the total surface area of all particles within the apparatus, heat transfer intensity increases significantly [23]. Such regenerators can be used to maintain the required temperature level in greenhouses [24].

Thermal energy storage (TES) technology has an indisputable advantage in addressing the intermittency of solar energy. The main challenge hindering the full exploitation of solar thermal

technologies for space heating (or cooling) and domestic hot water supply is related to the inherently variable nature of the energy source, with effective utilization depending on the availability of energy storage systems [25]. Engineering solutions require a multicriteria trade-off analysis based on key indicators such as heat source characteristics, power demand, spatial and weight constraints, and economic costs.

The aim of this study is to determine the energy performance characteristics of sensible heat storage systems employing a dense crushed-stone bed in a vertical heat-exchange channel, and of latent heat storage systems using a paraffin T3-based phase change material, for greenhouse applications.

MATHEMATICAL MODELS OF HEAT ACCUMULATION IN TES ELEMENTS

The study considers sensible heat storage (SHS) systems based on a dense bed of granular material and latent heat storage (LHS) systems using a phase change material (PCM), both designed for the accumulation of low-grade heat.

In developing the mathematical model of melting and solidification of the phase change material filling a cylindrical channel, the approximation of an infinitely long cylinder is adopted. This approximation is justified under the condition that the length of the actual cylinder is more than 50 times its radius, which is practically achievable. It is assumed that the paraffin is in a liquid state at a temperature t_0 exceeding the phase transition temperature t_p . Starting from a certain moment, a constant temperature $t_s < t_{ph}$ is established on its surface and maintained thereafter (first-type boundary condition). From this moment, the formation of a solidified layer begins, the thickness of which increases over time. The inner boundary of this layer, with a variable coordinate $\xi(\tau)$, represents the phase interface and maintains a constant temperature t_{ph} . At this boundary, the latent heat of phase transition L is released. Assuming constant physical properties of the material, the heat conduction differential equation in cylindrical coordinates is expressed as:

$$\frac{\partial t}{\partial \tau} = a \left(\frac{\partial^2 t}{\partial r^2} + \frac{1}{r} \frac{\partial t}{\partial r} + \frac{\partial^2 t}{\partial z^2} + \frac{1}{r^2} \frac{\partial^2 t}{\partial \varphi^2} \right). \quad (1)$$

where a is the thermal diffusivity coefficient (m^2/s), t is the temperature ($^{\circ}C$), and r, z, φ are the cylindrical coordinates.

It is assumed that the temperature along the cylinder axis and around the circumference remains constant, i.e., $\frac{\partial t}{\partial z} = \frac{\partial^2 t}{\partial z^2} = 0$,

$\frac{\partial t}{\partial \varphi} = \frac{\partial^2 t}{\partial \varphi^2} = 0$. Under these conditions, the temperature varies only along the radial direction r . Due to axial symmetry, the central line at $r=0$ is insulated; therefore, only half of the cylinder is considered for analysis. The thermophysical properties of the solid and liquid zones are assumed to be temperature-independent, and the densities in both zones are taken as equal ($\rho_s = \rho_l = \rho$). Taking these assumptions into account, the heat conduction differential equations for the solid and liquid states are expressed as:

$$\begin{cases} \frac{\partial t_s}{\partial \tau} = a \left(\frac{\partial^2 t_s}{\partial r^2} + \frac{1}{r} \frac{\partial t_s}{\partial r} \right) \\ \frac{\partial t_l}{\partial \tau} = a \left(\frac{\partial^2 t_l}{\partial r^2} + \frac{1}{r} \frac{\partial t_l}{\partial r} \right) \end{cases}. \quad (2)$$

Initial condition:

for $\tau = 0$: $t(r, 0) = t_0 = const$; $\xi(0) = 0$.

Boundary conditions:

for $r = 0, \tau > 0$: $t(0, \tau) = t_{surface} = const$.

Axial symmetry condition:

for $\tau > 0, r = 0$: $\frac{\partial t}{\partial r} = 0$.

Conditions at the phase interface:

a) temperature continuity condition:

at $r = \xi(\tau)$: $t_s(\xi, \tau) = t_l(\xi, \tau) = t_{ph} = const$;

b) equality of heat fluxes from the solid and liquid sides:

$$dQ_s = dQ_l + dQ_{ph}. \quad (3)$$

According to (3), the amount of heat removed by thermal conductivity from the phase boundary into the solid zone (dQ_s) is equal to the sum of the amount of heat entering due to thermal conductivity from the liquid zone (dQ_l) and the heat of phase transition released at the boundary (dQ_{ph}).

The condition at the phase interface follows from Fourier's law applied to the liquid and solid zones, taking into account the latent heat of phase transition:

$$-\lambda_s \left(\frac{\partial t_s}{\partial r} \right)_{-z} = -\lambda_l \left(\frac{\partial t_l}{\partial r} \right)_{+z} + L \cdot \rho \frac{d\xi}{d\tau} \quad (4)$$

where λ_s, λ_l are the thermal conductivities of the solid and liquid zones, respectively W/(m·K), and L is the specific latent heat of phase transition J/kg.

A similar problem was solved numerically by the authors of [26]. It should be noted that, in order to obtain temperature values from the derived relationships, the Stefan numbers are required, which must be determined experimentally.

In the mathematical modeling of a sensible heat storage system, the main component of which is an insulated channel filled with a dense bed of granular material, the contact heat transfer between the dense particle layer and the gas (or liquid) flow was considered. Under the adopted assumptions, the heat conduction equation takes the following form:

$$(1-\varepsilon) \cdot \rho_s \cdot c_s \cdot \frac{\partial t_s}{\partial \tau} = \lambda_s^* \cdot \frac{\partial^2 t}{\partial z^2} + \alpha(\bar{x}, \tau) \cdot a \cdot (t_l - t_s) \quad (5)$$

The effective thermal conductivity λ_s^* accounts for heat transfer by conduction within the particles (the material), through particle contacts, and across the fluid layer between them. Intercomponent heat exchange within the bed is taken into account using the corresponding heat transfer coefficient α , the value of which is determined experimentally.

To obtain a solution, instead of temperature, the excess temperature $\mathcal{G} = t_l - t_s$ is introduced

$$C_n = \frac{2\mathcal{G}_0 \cdot \sin\left(\frac{\sqrt{\gamma \cdot k_i^2 + \alpha \cdot f_{ssa}} \cdot Z}{\sqrt{\gamma}}\right) \cdot \sqrt{\gamma}}{\cos\left(\frac{\sqrt{\gamma \cdot k_i^2 + \alpha \cdot f_{ssa}} \cdot Z}{\sqrt{\gamma}}\right) \cdot \sin\left(\frac{\sqrt{\gamma \cdot k_i^2 + \alpha \cdot f_{ssa}} \cdot Z}{\sqrt{\gamma}}\right) \cdot \sqrt{\gamma} + \sqrt{\gamma \cdot k_i^2 + \alpha \cdot f_{ssa}} \cdot Z} \quad (8)$$

For the roots of the characteristic equation, corresponding tables of $k=f(Bi)$ were compiled. Model verification showed that the calculated data correlate satisfactorily with experimental results obtained under similar conditions. However, the intercomponent heat transfer coefficients, which must be specified as input data, can only be determined experimentally. It

into equation (5). Then, equation (5) is transformed into the following form (6):

$$(1-\varepsilon) \cdot \rho_s \cdot c_s \cdot \frac{\partial \mathcal{G}}{\partial \tau} = \lambda_s^* \cdot \frac{\partial^2 \mathcal{G}}{\partial z^2} + \alpha(\bar{x}, \tau) \cdot a \cdot \mathcal{G} \quad (6)$$

The following uniqueness conditions are adopted:

- 1) geometrical: channel length Z;
- 2) physical: $\lambda = \text{const}, c = \text{const}, a = \text{const}$;
- 3) initial: at $\tau = 0, \mathcal{G} = \mathcal{G}_0; \mathcal{G}_0 = t_l - t_s$;
- 4) boundary condition: for $\tau > 0, z = 0$:

$$\frac{\partial \mathcal{G}}{\partial z} = 0;$$

- 5) boundary at the contact surface between the solid particle layer and the fluid:

$$-\lambda_s^* \left(\frac{\partial \mathcal{G}}{\partial z} \right)_{z=\delta} = \alpha \cdot (1-\varepsilon) \cdot \mathcal{G}.$$

The solution of equation (6) was obtained using the method of separation of variables with Maple 2025.1 software:

$$\mathcal{G} = \sum_{n=1}^{n \rightarrow \infty} C_n \cdot \frac{\sqrt{a \cdot c \cdot \rho \cdot k_i^2 + \alpha \cdot f_{ssa}}}{\sqrt{a \cdot c \cdot \rho}} \cdot \cos\left(\frac{\sqrt{a \cdot c \cdot \rho \cdot k_i^2 + \alpha \cdot a_{y0}}}{\sqrt{a \cdot c \cdot \rho}} z\right) \cdot e^{-\frac{a \cdot k_i^2 \cdot \tau}{\beta}} \quad (7)$$

where f_{ssa} – specific surface area of particles per unit volume, $\gamma = a \cdot c \cdot \rho$ and the constants C_n are determined from the relation (8):

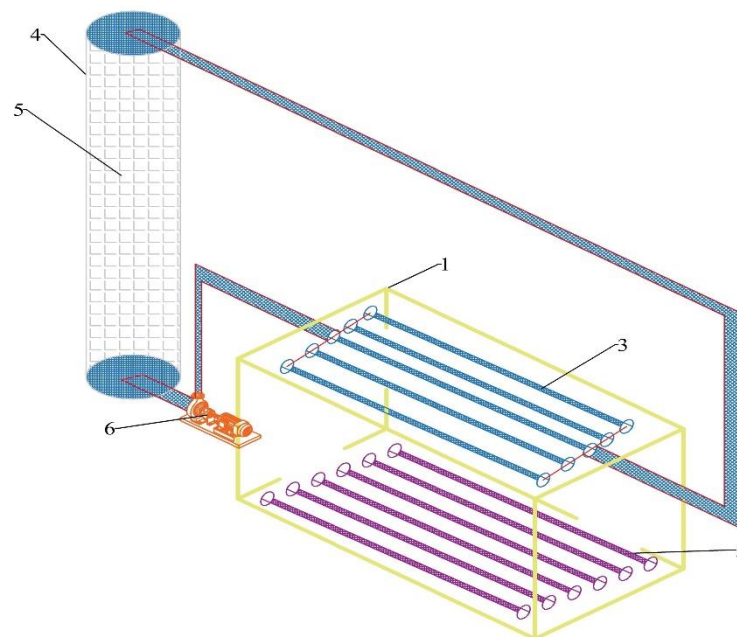
should also be noted that the presented mathematical models adopt first-type boundary conditions $t=\text{const}$, which, when modeling accumulation processes in greenhouse conditions, are valid only for limited time intervals. Therefore, the application of these mathematical models is suitable for estimating the performance characteristics of thermal storage units and for use

in conjunction with additional data obtained from experimental studies.

MATERIALS AND METHODS

To investigate the performance of TES systems, an experimental setup in the form of a greenhouse mock-up was fabricated and tested. The setup included a crushed-stone layer for sensible heat storage, tubes containing a phase change material undergoing a solid-liquid transition, as well as control and measurement instrumentation. The dimensions of the greenhouse mock-up were determined using the method of similarity theory. A schematic of the experimental setup is shown in Fig. 1.

- The main components of the setup included:
- the greenhouse body mock-up (1) with overall dimensions of $0.5 \times 1.0 \times 0.5$ m, made of acrylic glass;
 - polymer tubes (2) filled with paraffin, placed directly on the greenhouse floor;
 - an insulated channel (4) containing a dense crushed-stone layer (5);
 - a polymer tube (3) with a diameter of 2 cm, forming a closed loop through which water circulates;
 - a pump (6) designed for water circulation.



1 – greenhouse body mock-up, 2 – heat storage tubes with modified paraffin, 3 – water circulation heating loop, 4 – heat-exchange channel, 5 – dense crushed-stone layer, 6 – liquid pump

Fig. 1. Schematic of the experimental setup for investigating the efficiency of low-grade solar heat accumulation.

In the sensible heat storage system, a water circulation loop is organized, serving as an intermediate heat carrier. Directly beneath the greenhouse roof, polymer channels carry water, which is heated by solar radiation during the daytime. After being heated under the roof, the water is delivered to the upper section of a vertical, insulated heat-exchange channel filled with crushed stone. As the water flows around the crushed-stone particles, heat transfer occurs. At the outlet of the heat-exchange channel, a pump returns the cooled water to the channels beneath the greenhouse roof, where it is reheated. The vertical arrangement of the crushed-stone heat-

exchange channel and its inclusion in a closed circulation loop is justified by the need to reduce pressure losses as the heat carrier passes through the dense particle bed. As demonstrated in previous studies of a soil-based regenerator [23], the length of the heat-exchange channel is limited by the ability of fans to overcome the aerodynamic resistance of the particle layer. The proposed configuration overcomes this problem: water moves downward through the heat-exchange section under the influence of gravity, and heat is transferred upon contact with the particle layer.

For a comparative assessment of capacity-type TES and phase change material (PCM) – based TES, tubes filled with modified paraffin T3 were placed on the greenhouse floor. Commercially available paraffin grades have phase transition temperatures of 50 °C and above, making them unsuitable as storage materials for greenhouse applications. To lower the phase transition temperature, vaseline oil and glycerin were added to the melted paraffin T3. As a result, the melting temperature decreased to $t_{\text{melt}}=35$ °C, although the specific latent heat of fusion was reduced.

The experiment monitored the following parameters: the temperature of the water circulating through the transparent channel on the greenhouse roof and heated by solar radiation; the temperature of the crushed-stone layer at three points along the height of the heat-exchange channel; the temperature of the paraffin in the polymer tubes; and the ambient temperature. Temperature measurements were carried out using DS18B20 thermocouples. The intensity of solar radiation was determined by calculation based on readings from a digital light sensor (GY-302 BH1750FVI). For sunlight on a clear day, an approximate conversion factor of $120,000 \text{ lx} \approx 1000 \text{ W/m}^2$ is recommended.

To enable continuous monitoring of temperature and illumination, an automated data collection, storage, and transmission system was developed, based on an Arduino Mega 2560 R3 controller, an ESP32 module, and a Raspberry Pi 5 mini-computer, each performing different but interrelated functions. Pump operation was controlled automatically based on the sensor readings.

The measurement system consists of the following levels:

1. Sensor level – measurement of physical parameters of the environment and the heat-accumulating materials.
2. Controller level (Arduino Mega 2560 R3) – data processing and control.
3. Server level (Raspberry Pi 5) – data collection, storage, and visualization.
4. Power module – autonomous supply from solar panels and a battery.

The rationale for integrating these modules into a single system is as follows:

- the Arduino module performs low-level control and management functions, while the Raspberry Pi handles resource-intensive tasks such as processing, storage, and visualization. This prevents overloading a single device.

- increased reliability: In the event of Wi-Fi loss or server failure, the Arduino continues to autonomously record data to an SD card. Once connectivity is restored, the data are synchronized, preventing information loss.

- flexibility and scalability: The architecture can be easily expanded—new sensors or actuators can be added, or additional greenhouses can be connected, each with separate Arduino and ESP32 units sending data to the common server.

- energy efficiency and autonomy: Powered by solar panels and a battery, the system can operate fully autonomously without connection to a 220 V mains supply, which is especially important for remote sites.

Modularity: Each system node performs a clearly defined task, simplifying maintenance, repair, and system upgrades.

All physical parameters were measured at 10-second intervals. The collected data were used to analyze thermal processes in individual components of the setup (the heat-exchange channel, paraffin, and the air inside the greenhouse mock-up), to evaluate the efficiency of heat accumulation, and to assess its potential utilization.

The energy subsystem provides autonomous electrical power to the entire experimental setup. The subsystem consists of two 100 W solar panels, a solar charge controller, a 12 V 13 Ah battery, and a power distribution module supplying 5 V and 3.3 V to the controllers and sensors. The solar panels used are monocrystalline, featuring high-efficiency photovoltaic cells and a flexible design. The panels were connected in parallel, maintaining a voltage range of 12–18 V with a total current of up to 11 A (under maximum illumination). On a clear sunny day, the combined output of the two 200 W panels provided:

- a battery charging current of approximately 10–11 A at 14 V,
- a daily energy generation of up to 1.2–1.4 kWh.

This was sufficient to fully charge the 13 Ah battery in 2–3 hours of strong sunlight and to continuously power the entire setup (total consumption around 15–20 W) for 24 hours, including periods of autonomous operation at night. Thus, the 200 W solar energy subsystem ensures stable power supply to all system components (Arduino, ESP32, Raspberry Pi 5, pump); 24-hour operation without an external power source; resilience to external climatic

conditions; continuous monitoring and data transmission, even in remote locations.

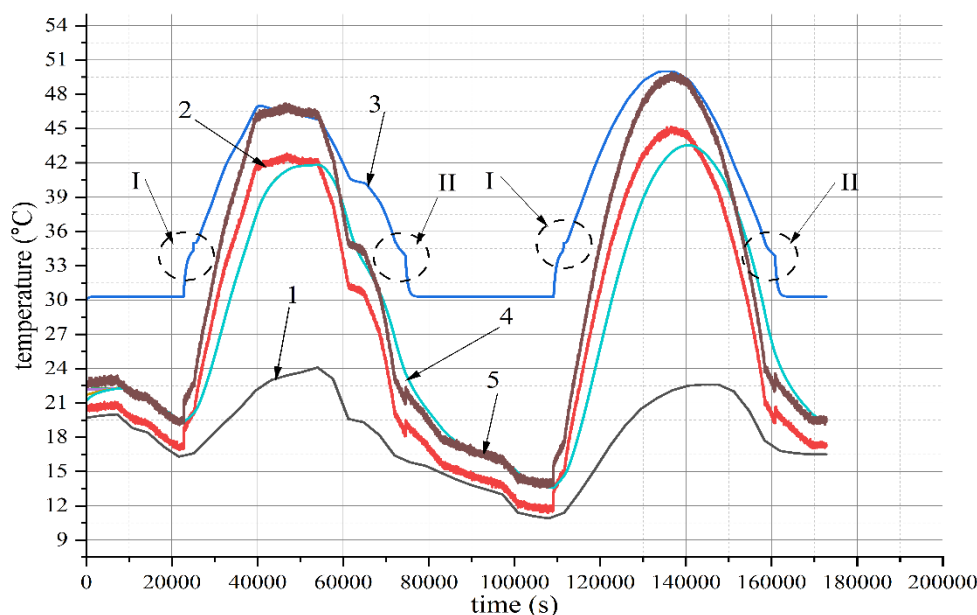
RESULTS AND DISCUSSION

The temperature profiles of the heat-accumulating materials, greenhouse air, ambient air, and water in the circulation loop, measured over a two-day period, are shown in Fig. 2. Starting from the period 21,700–22,777 s (around 6 a.m.), the intensity of solar radiation increased, leading to a rise in all measured temperatures. The outdoor air temperature (curve 1) was significantly lower than the air temperature inside the greenhouse (curve 2), which can be explained by the insulated nature of the greenhouse airspace. The temperature of the phase change material (modified paraffin, curve 3) was consistently higher than that of the water, crushed stone, and greenhouse air because the paraffin-filled tubes were positioned directly on the greenhouse floor. Observations showed that the floor temperature of the greenhouse mock-up did not fall below 30 °C during the night, indicating the high heat-

accumulating capacity of the floor material itself. On this curve, the regions of phase transition during melting (I) and solidification (II) of the modified paraffin are highlighted separately.

It can be seen that the temperature of the layer (curve 3) correlates with the temperature of the water flow (curve 5), remaining lower. At the upper point of the graph, the temperature difference reached its maximum: $\Delta t=3,5$ °C. On the second day, the maximum temperature difference was higher due to increased solar radiation intensity, reaching $\Delta t=4,5$ °C.

The temperature of the water flowing through the tubes beneath the greenhouse roof remained higher than the air temperature inside the greenhouse throughout the study: during the day, because the transparent polyethylene tubes laid directly on the roof allowed the solar radiation to heat the water flow, and at night, because the water received heat from the crushed-stone layer as it passed through it.



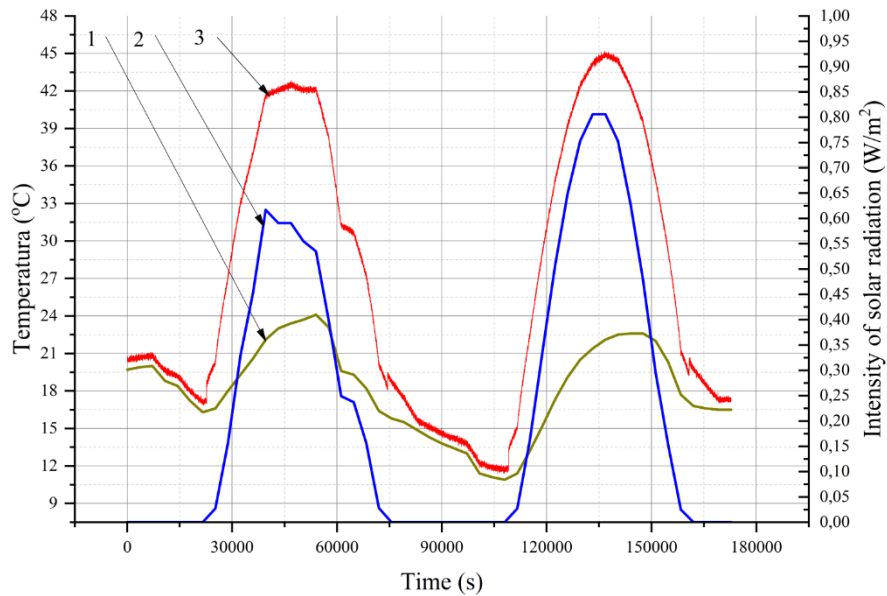
1 – ambient air temperature, 2 – air temperature in the greenhouse mock-up, 3 – paraffin temperature in the phase change material storage tubes, 4 – average temperature of the crushed-stone particles in the upper part of the heat-exchange channel, 5 – water temperature at the outlet of the greenhouse body

I – solid-to-liquid phase transition, II – liquid-to-solid phase transition

Fig. 2. Temperature profiles of the working media during the experiment.

For comparative analysis, Fig. 3 shows the temperature profiles of the greenhouse air, the ambient environment, and the solar radiation intensity curve. Changes in the air temperature

within the greenhouse volume and in the surrounding environment are determined by the intensity of solar radiation, as illustrated in Fig. 3.



1 – ambient air temperature, 2 – solar radiation intensity, 3 – air temperature in the greenhouse
Fig. 3. Changes in air temperature inside the greenhouse mock-up and in the surrounding environment as a function of solar radiation intensity.

It can be observed (Fig.3) that while the outdoor air temperature did not exceed 24 °C during the day, the air temperature inside the greenhouse mock-up reached 42–45 °C. This highlights the need to reduce it to create conditions suitable for greenhouse operations.

The temperature and illumination curves shown in Figs.2 and 3 were analyzed and processed using OriginPro 2024 software. The resulting dependencies are presented in Table 1.

Analysis of the curves and the generalized functions showed that the temperature variations of the particle layer and the water in the circulation loop are described by a single GaussAmp function. Thus, there is a strict correlation between the variables, where each value of one variable corresponds to a specific value of the other. This allows the behavior of one parameter to be predicted based on the values of the other using mathematical modeling.

The vertical arrangement of the crushed-stone heat-exchange channel and the organization of heat transfer with water supplied from above solved the problem of hydraulic resistance in the layer. Moreover, switching from an air-based to a water-based heat carrier led to a significant

increase in the intercomponent heat transfer coefficient α . For air under similar conditions, $\alpha=17$, whereas for water, based on the results of this experiment, $\alpha=80$. The obtained value of the intercomponent heat transfer coefficient makes it possible to calculate the temperature distribution within the layer along its height.

To assess energy efficiency, thermal calculations were carried out based on experimental data of the working media temperatures. The amount of heat accumulated by the crushed-stone layer in the heat-exchange channel during the period of increasing solar radiation intensity, assuming no heat losses to the environment, was determined using the following formula:

$$Q = m \cdot c \cdot \Delta t, \text{ J.} \quad (9)$$

where m , c are the mass and specific heat capacity of the crushed stone, respectively $m=40$ kg, $c=800$ J/(kg·K), and Δt is the temperature change of the crushed-stone layer as it is heated by the water flow from the circulation loop.

Table 1

Summary of empirical temperature and illumination curves as a function of time.
 f – type of function, ε – relative error.

Day	Process	Generalized dependence	f	ε , %
1	Heating/cooling of water in the circulation loop	$t_{w1} = 15.7 + 32.6 \cdot \exp(-0.5 \cdot ((\tau - 47841) / 14939)^2)$, °C	GaussAmp	3.6
2		$t_{w2} = 12.16 + 38.5 \cdot \exp(-0.5 \cdot ((\tau - 137032) / 15593)^2)$, °C		3.1
1	Heating/cooling of crushed stone in the heat-exchange column	$t_{g1} = 17.6 + 24.3 \cdot \exp(-0.5 \cdot ((\tau - 53570) / 14026)^2)$, °C	GaussAmp	8.8
2		$t_{g2} = 2.9 + 41.0 \cdot \exp(-0.5 \cdot ((\tau - 140848) / 19296)^2)$, °C		3.9
1	Heating/cooling of paraffin in the greenhouse mock-up	$t_{p1} = 15.3 + 31.7 \cdot \exp(-0.5 \cdot ((\tau - 45341) / 20768)^2)$, °C	GaussAmp	2.6
2		$t_{p2} = 12.7 + 37.4 \cdot \exp(-0.5 \cdot ((\tau - 135249) / 22952)^2)$, °C		2.0
1	Heating/cooling of air in the greenhouse mock-up	$t_{a1} = 13.6 + 30.2 \cdot \exp(-0.5 \cdot ((\tau - 47768) / 14877)^2)$, °C	GaussAmp	7.1
2		$t_{a2} = 10.2 + 42.1 \cdot \exp(-0.5 \cdot ((\tau - 143278) / 25278)^2)$, °C		4.5
1	Illumination	$E_1 = 72760 / (1 + 31670 / \tau)^{13.8} / (1 + \tau / 60963)^{15.26}$, lx	BiHill	4.1
2		$E_2 = 100218 / (1 + 120699 / \tau)^{31.0} / (1 + \tau / 148617)^{39.5}$, lx		1.6

Heat losses to the environment can be neglected because the heat-exchange channel is effectively insulated externally with a 5 mm layer of chemically cross-linked polyethylene foam, covered on the outside with aluminum foil. On the first day, the amount of accumulated heat was $Q=736000$ J, and on the second day it was $Q=912000$ J. The increase in accumulated heat on the second day is associated with the higher intensity of solar radiation, while the heating started from a lower initial temperature than on the first day (Fig. 3). Calculations showed that a 1.27-fold increase in the average integrated solar radiation intensity led to a 1.24-fold increase in accumulated heat. The specific heat accumulated per kilogram of crushed stone is $Q_s=18400\dots22800$ J/kg. After the peak temperature of the crushed-stone layer is reached, it is proposed to stop the water supply and insulate the heat-exchange channel at the inlet and outlet with shutters. During nighttime temperature drops in the greenhouse, the accumulated heat is intended to be utilized to raise the air temperature.

The amount of heat accumulated by a single channel with modified paraffin during the heating period was determined using the following relation:

$$Q = m_{par} \cdot c \cdot \Delta t_1 + m_{par} \cdot L + m_{par} \cdot c_p \cdot \Delta t_2. \quad (10)$$

where m_{par} is the mass of paraffin in the channel, Δt_1 is the temperature change of the paraffin in the solid state, Δt_2 is the temperature change of the paraffin in the liquid state, L is the latent heat of fusion, c is the specific heat capacity of the paraffin in the solid state, and c_p is the specific heat capacity in the liquid state. The length of the paraffin storage tube is 1 m, with an internal diameter of 2 cm.

Analyzing the temperature curve of the paraffin (Fig. 2), it can be concluded that its heat capacity in the solid and liquid states is practically the same and does not depend on temperature within this range. In this case, relation (2) can be expressed in the following form:

$$Q = m_{par} \cdot c \cdot \Delta t + m_{par} \cdot L. \quad (11)$$

where Δt is the temperature change over the entire heating period.

The mass of modified paraffin in a 1 m long channel with a diameter of 0.02 m in the experiment was 0.283 kg. Its temperature increased from 30 °C to 46 °C over the entire heating period, as shown in Fig. 3. The phase transition from solid to liquid occurred at 34–

35.5 °C (Fig. 2) over a short time interval, which is reflected in the temperature curve.

As a result of the calculation, the amount of heat accumulated by the modified paraffin was found to be $Q=48450$ J. The calculation assumed a specific heat capacity of the paraffin $c=2200$ J/(kg·K) and a latent heat of fusion for the modified paraffin $\lambda=134$ kJ/kg. Six channels were installed at the floor of the greenhouse mock-up; accordingly, the total accumulated heat was $Q=290700$ J. The specific amount of heat accumulated was $Q_s=171200$ J/kg.

From the temperature curves of the paraffin and the solar radiation intensity during the phase transition period, the emissivity of the storage tubes, made of nylon, can be estimated. The duration of this period (Fig. 2) was $\tau=1800$ s, and the average solar radiation intensity was $I=550$ W/m². Taking into account the surface area of the heat storage tubes, the incident thermal flux was $Q=207$ W. The heat absorbed by the phase change material was $Q=126$ W. For these values, the effective emissivity is $\varepsilon_{\text{eff}}=0.61$.

Considering the greenhouse mock-up as a system of flat-parallel bodies (a flat acrylic roof and the floor with small-diameter storage tubes) and assuming the emissivity of the acrylic glass is $\varepsilon_g=0.92$, the emissivity of the surface of the paraffin-filled storage tubes was determined as $\varepsilon_s=0.65$. This value is necessary for performing engineering calculations of open-type phase change material storage units, i.e., those exposed directly to solar radiation.

The data from Figs. 2 and 3 allow for estimating the mass of modified paraffin required to thermally stabilize the internal volume of the greenhouse mock-up. For the measured solar radiation intensity, taking into account heat losses to the environment, the paraffin mass should be no less than 25.5 kg/m³. In the actual experiment, only 1.7 kg was used, which resulted in a continuous increase in the temperature of both the material and the air inside the greenhouse. It should also be noted that during regular greenhouse operation, the radiation intensity may be lower, so the calculated mass represents the maximum required. However, there arises the issue of accommodating such a volume of phase change material within the greenhouse interior, necessitating alternative design solutions.

By comparing the specific amounts of heat accumulated by the crushed-stone layer and the phase change material, it can be concluded that the phase change material accumulates low-grade heat 7.5–9.3 times more efficiently. At the same

time, the mass of the modified paraffin used is 23.6 times smaller than that of the crushed stone. However, situating the crushed-stone heat-exchange channel outside the greenhouse is preferable compared to placing the paraffin storage tubes on the ground, as it does not reduce the usable greenhouse area. Furthermore, as seen in Fig. 2, the paraffin temperature was higher than the air temperature. Efficient operation of the phase change storage can be achieved by enclosing the tubes in a casing made of a solar-transparent material with low thermal conductivity. In this configuration, solar radiation will be absorbed by the phase change material without heating the greenhouse air.

Thus, installing crushed-stone heat-exchange channels has an advantage for existing greenhouses, as it does not require a major redesign. For newly constructed greenhouses, it is rational to provide for a regenerative heat-exchanger utilizer with phase change material, which requires additional design development.

CONCLUSION

The use of a dense crushed-stone layer in a heat-exchange channel is an effective solution for a low-grade explicit heat storage system (SHS). The average intercomponent heat transfer coefficient between the circulating water and the crushed-stone layer is $\alpha=80$ W/(m²·K).

The installation of a vertical, thermally insulated channel with crushed stone and the supply of water to its upper part—after heating in the greenhouse body from low-grade heat sources—eliminates the problem of hydraulic resistance in the dense layer. The specific amount of heat accumulated per kilogram of crushed stone under the experimental conditions was $Q_s=18400\dots22800$ J/kg.

Modified paraffin T3, as a phase change material, accumulates low-grade heat from solar radiation and greenhouse air 7.5–9.3 times more efficiently than a dense crushed-stone layer; however, integrating a phase change material system requires design development that accounts for the operational characteristics of the greenhouse.

To thermally stabilize the internal volume of the greenhouse mock-up at 33–35 °C under an average solar radiation intensity of $I=550$ W/m², the mass of modified paraffin should be no less than 25 kg of paraffin per cubic meter of the greenhouse volume.

The emissivity of the surface of the nylon storage tubes with paraffin is $\varepsilon_s=0.65$.

The final choice of a heat storage system depends on the material and manufacturing costs of the TES system, the simplicity of the design, and the feasibility of integration within the greenhouse volume.

ACKNOWLEDGMENTS

This research was made thanks to the funding from the National Research Foundation of Ukraine for the research project "Solving fundamental problems of creating a new generation of thermal storage nanomaterials for storing solar energy and waste heat (thermophysical properties, heat transfer)" (Registration No. 2025.07/0417).

REFERENCES

- [1] Horzela-Miś A., Semrau J. (2025). The role of renewable energy and storage technologies in sustainable development: simulation in the construction industry. *Frontiers in Energy Research*, 2025, vol. 13, pp. 1-14. doi: [10.3389/fenrg.2025.1540423](https://doi.org/10.3389/fenrg.2025.1540423).
- [2] Ali H.M., Rehman T.-u., Arıcı M., Said Z., Duraković B., Mohammed H.I., Kumar R., Rathod M.K., Buyukdagli O., Teggat M. Advances in thermal energy storage: Fundamentals and applications. *Progress in Energy and Combustion Science*, 2024, 100: 101109. doi: [10.1016/j.pecs.2023.101109](https://doi.org/10.1016/j.pecs.2023.101109).
- [3] Mitali J., Dhinakaran S., Mohamad A.A. Energy storage systems: a review. *Energy storage and saving*. 2022, vol. 1, pp. 166-216. doi: [10.1016/j.enss.2022.07.002](https://doi.org/10.1016/j.enss.2022.07.002).
- [4] Ji D., Liu G., Romagnoli A., Rajoo S., Besagni G., Markides C.N. Low-grade thermal energy utilization: Technologies and applications. *Applied Thermal Engineering*, 2024, vol. 244, 122618. doi: [10.1016/j.applthermaleng.2024.122618](https://doi.org/10.1016/j.applthermaleng.2024.122618).
- [5] Schwarzmayr P., Birkelbach F., Walter H., Hofmann R. Standby efficiency and thermocline degradation of a packed bed thermal energy storage: An experimental study. *Applied Energy*, 2023, vol. 337, 120917. doi: [10.1016/j.apenergy.2023.120917](https://doi.org/10.1016/j.apenergy.2023.120917).
- [6] Audu G.A., Mafo A.R., Jegede R.E., Tarasenko M., Kozak K. Advances in energy storage technologies for renewable energy systems: bridging intermittency and sustainable integration. *Eurasian Journal of Physics and Functional Materials*, 2025, vol. 9, no. 2, pp. 79–96. doi: [10.69912/2616-8537.1243](https://doi.org/10.69912/2616-8537.1243).
- [7] Suresh C., Saini R.P. Thermal performance of sensible and latent heat thermal energy storage systems. *International Journal of Energy Research*, 202, vol. 44, no. 6, pp. 4743–4758. doi: [10.1002/er.5255](https://doi.org/10.1002/er.5255).
- [8] Bazgaou A., Fatnassi H., Bouharroud R., Elame F., Ezzaeri K., Gourdo L., Wifaya A., Demrati H., Tiskatine R., Bekkaoui A., Aharoune A., Bouirden L. Performance assessment of combining rockbed thermal energy storage and water filled passive solar sleeves for heating Canarian green-house. *Solar Energy*, 2020, vol. 198, pp. 8–24. doi: [10.1016/j.solener.2020.01.041](https://doi.org/10.1016/j.solener.2020.01.041).
- [9] Katekar V.P., Rao A.B., Sardeshpande V.R. An experimental investigation to optimise pebbles-based sensible heat storage system: An exploration to improve thermal efficiency of solar devices. *Journal of Energy Storage*, 2023, vol. 73, 108964. doi: [10.1016/j.est.2023.108964](https://doi.org/10.1016/j.est.2023.108964).
- [10] Olivkar P.R., Katekar V.P., Deshmukh S.S., Palatkar S.V. Effect of sensible heat storage materials on the thermal performance of solar air heaters: State-of-the-art review. *Renewable and Sustainable Energy Reviews*, 2022, vol. 157, 112085. doi: [10.1016/j.rser.2022.112085](https://doi.org/10.1016/j.rser.2022.112085).
- [11] Peer M.S., Cascetta M., Migliari L., Petrollese M. Nanofluids in Thermal Energy Storage Systems: A Comprehensive Review. *Energies*, 2025, vol. 18, no. 3, 707. doi: [10.3390/en18030707](https://doi.org/10.3390/en18030707).
- [12] Bonachela S., López J.C., Granados M.R., Magán J.J., Hernández J., Baille A. Effects of gravel mulch on surface energy balance and soil thermal regime in an unheated plastic green-house. *Biosystems Engineering*, 2020, vol. 192, pp. 1–13. doi: [10.1016/j.biosystemseng.2020.01.010](https://doi.org/10.1016/j.biosystemseng.2020.01.010).
- [13] Cano-Pleite E., Hernández-Jiménez F., García-Gutiérrez L.M., Soria-Verdugo A. Thermo-economic optimization of a novel confined thermal energy storage system based on granular material. *Applied Thermal Engineering*, 2023, vol. 224, 120123. doi: [10.1016/j.applthermaleng.2023.120123](https://doi.org/10.1016/j.applthermaleng.2023.120123).
- [14] Singh H., Saini R.P., Saini J.S. A review on packed bed solar energy storage systems. *Renewable and sustainable energy reviews*, 2010, vol. 14, no. 3. pp. 1059–1069. doi: [10.1016/j.rser.2009.10.022](https://doi.org/10.1016/j.rser.2009.10.022).
- [15] Singh H., Saini R.P., Saini J.S. A review on packed bed solar energy storage systems. *Renewable and sustainable energy reviews*, 2010, vol. 14, no. 3, pp. 1059–1069. doi: [10.1016/j.rser.2009.10.022](https://doi.org/10.1016/j.rser.2009.10.022).
- [16] Mastouri H., Benhamou B., Hamdi H. Pebbles Bed Thermal Storage for Heating and Cooling of Buildings. *Energy Procedia*, 2013, vol. 42, pp. 761–764. doi: [10.1016/j.egypro.2013.11.079](https://doi.org/10.1016/j.egypro.2013.11.079).
- [17] Faraj K., Khaled M., Faraj J., Hachem F., Castelain C. A review on phase change materials for thermal energy storage in buildings: Heating and hybrid applications. *Journal of Energy Storage*, 2021, vol. 33, 101913. doi: [10.1016/j.est.2020.101913](https://doi.org/10.1016/j.est.2020.101913).
- [18] Zhang Y., Guo Y., Zhu J., Yuan W., Zhao F. New Advances in Materials, Applications, and Design Optimization of Thermocline Heat Storage: Comprehensive Review. *Energies*, 2024, vol. 17, no. 10, 2403. doi: [10.3390/en17102403](https://doi.org/10.3390/en17102403).
- [19] Suresh C., Saini R.P. An experimental study on the performance evaluation of a combined sensible-

latent heat thermal energy storage. *International Journal of Energy Research*, 2020, vol. 45, no. 4, pp. 1-17. doi: [10.1002/er.6196](https://doi.org/10.1002/er.6196).

[20] Savytskyi M., Danishevskyy V., Bordun M. Accumulation of solar energy to heat greenhouses. *IOP conference series: materials science and engineering*, 2020, vol. 985. P.012013. doi: [10.1088/1757-899x/985/1/012013](https://doi.org/10.1088/1757-899x/985/1/012013).

[21] Bouadila S., Lazaar M., Skouri S., Kooli S., Farhat A. Assessment of the greenhouse climate with a new packed-bed solar air heater at night, in Tunisia. *Renewable and Sustainable Energy Reviews*, 2014, vol. 35, pp. 31–41. doi: [10.1016/j.rser.2014.03.051](https://doi.org/10.1016/j.rser.2014.03.051).

[22] Solodka A., Volgusheva N., Boshkova I., Titlov A., Rozhentsev A. Investigation of heat exchange in a blown dense layer of granular materials. *Eastern-European Journal of Enterprise Technologies*, 2017, vol. 5, no. 8, pp. 58–64. doi: [10.15587/1729-4061.2017.112217](https://doi.org/10.15587/1729-4061.2017.112217).

[23] Mukminov I., Volgusheva N., Georgiesh C., Boshkova I. Experimental study of a pilot unit of a

ground regenerator for greenhouses. *ScienceRise*, 2022, vol. 2, pp. 3–10. doi: [10.21303/2313-8416.2022.002411](https://doi.org/10.21303/2313-8416.2022.002411)

[24] Soussi M., Chaibi M.T., Buchholz M., Saghrouni Z. Comprehensive Review on Climate Control and Cooling Systems in Greenhouses under Hot and Arid Conditions. *Agronomy*, 2022, vol. 12, no. 3, pp. 1-31. 626. doi: [10.3390/agronomy12030626](https://doi.org/10.3390/agronomy12030626).

[25] Mao Q., Wang, Y. Recent development of thermal heat storage technology coupling with phase change material. *Journal of Energy Storage*, 2025, vol. 139, 118739. doi: [10.1016/j.est.2025.118739](https://doi.org/10.1016/j.est.2025.118739).

[26] Barannyk L., Crepeau J., Paulus P., Siahpush A. Fourier-Bessel Series Model for the Stefan Problem With Internal Heat Generation in Cylindrical Coordinates. *Proceedings of the 2018 26th International Conference on Nuclear Engineering ICONE26 July 22-26 2018, London, England*, <https://doi.org/10.1115/icone26-81009>.

Information about authors.



Igor Mukminov, PhD, Senior Lecturer. Scientific interests: heat transfer in granular media and automation of experimental data acquisition.

E-mail: fatalrew@gmail.com

ORCID: <https://orcid.org/0000-0002-3674-9289>



Volgusheva Natalya, Candidate of Technical Sciences (Ph.D.), Associate Professor. Scientific interests: heat and mass transfer in dense and dispersed layers.

E-mail: natvolgusheva@gmail.com

ORCID: <https://orcid.org/0000-0002-9984-6502>



Verkhivker Yakov, Doctor of Technical Sciences, Professor. Scientific interests: technological development of process flow solutions for the production of final consumer products across various industries.

E-mail: yaverkhivker@gmail.com

ORCID: <https://orcid.org/0000-0002-2563-4419>



Igor Pysarevskiy, Master's degree. Scientific interests: interdisciplinary intersection of chemistry, energy, and heat and mass transfer. Graduate student.

E-mail: rori@ukr.net

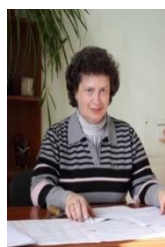
ORCID: <https://orcid.org/0009-0007-3920-9601>



Irina Boshkova, Doctor of Technical Sciences, Professor. Scientific interests: processes of heat and mass transfer in dense and dispersed layers with different methods of heat supply.

E-mail: boshkova.irina@gmail.com

ORCID: <https://orcid.org/0009-0009-5599-2709>



Altman Ella, Candidate of Technical Sciences (Ph.D.), Associate Professor. Scientific interests: hydromechanics of single-phase and two-phase flows, modeling of thermohydrodynamic processes, and cooling systems.

E-mail: altman.ella.i@gmail.com

ORCID: <https://orcid.org/0000-0002-8934-2036>